



Published in final edited form as:

*Nat Chem Biol.* 2020 January ; 16(1): 95–103. doi:10.1038/s41589-019-0392-5.

## Site-specific acylation of a bacterial virulence regulator attenuates infection

Zhenrun J. Zhang<sup>1</sup>, Virginia A. Pedicord<sup>1,2</sup>, Tao Peng<sup>1,3</sup>, Howard C. Hang<sup>1,\*</sup>

<sup>1</sup>Laboratory of Chemical Biology and Microbial Pathogenesis, The Rockefeller University, New York, New York, United States.

<sup>2</sup>Department of Medicine, University of Cambridge, Cambridge, United Kingdom.

<sup>3</sup>School of Chemical Biology and Biotechnology, Peking University Shenzhen Graduate School, Shenzhen, Guangdong, China.

### Abstract

Microbiota generates millimolar concentrations of short-chain fatty acids (SCFAs) that can modulate host metabolism, immunity and susceptibility to infection. Butyrate in particular can function as a carbon source and anti-inflammatory metabolite, but the mechanism by which it inhibits pathogen virulence has been elusive. Using chemical proteomics, we discovered that several virulence factors encoded by *Salmonella* pathogenicity island-1 (SPI-1) are acylated by SCFAs. Notably, a transcriptional regulator of SPI-1, HilA, was acylated on several key lysine residues. Subsequent incorporation of stable butyryl-lysine analogs using CRISPR-Cas9 gene editing and unnatural amino acid mutagenesis revealed that site-specific modification of HilA impacts its genomic occupancy, expression of SPI-1 genes and attenuates *Salmonella enterica* serovar Typhimurium invasion of epithelial cells as well as dissemination *in vivo*. Moreover, a multiple-site HilA lysine-acylation mutant strain of *S. Typhimurium* was resistant to butyrate-mediated suppression *in vivo*. Our results suggest prominent microbiota-derived metabolites may directly acylate virulence factors to inhibit microbial pathogenesis *in vivo*.

### Introduction

Short-chain fatty acids (SCFAs) generated by gut microbiota fermentation of dietary polysaccharides exhibit significant effects on host physiology and immunity<sup>1</sup>. SCFA concentrations in the mammalian gut range from 1 – 100 mM<sup>2</sup>, depending on the location in the intestine, host diet and microbiota composition. Specific microbiota reconstitution studies have revealed that *Clostridia* cluster IV, XIVa, XVIII are key bacterial species involved in SCFA fermentation in the gut<sup>3</sup>. Amongst the SCFAs generated *in vivo*, butyrate has been reported to function as a nutrient source for colonocytes<sup>4</sup>, and as an agonist

Users may view, print, copy, and download text and data-mine the content in such documents, for the purposes of academic research, subject always to the full Conditions of use: [http://www.nature.com/authors/editorial\\_policies/license.html#terms](http://www.nature.com/authors/editorial_policies/license.html#terms)

\*Correspondence to: [hhang@rockefeller.edu](mailto:hhang@rockefeller.edu).

**Author contributions:** H.C.H. conceptualized the project, Z.J.Z. and V.P. performed experiments and data analysis, T.P. synthesized bmK, Z.J.Z. and H.C.H. wrote the paper, and all authors contributed to manuscript editing.

**Competing interests:** Authors declare no competing interests.

for G protein-coupled receptors (GPCRs: GPR41, GPR43, GPR109A) in multiple cell types<sup>5-9</sup> to maintain intestinal barrier function. Moreover, butyrate has been suggested to function as a lysine deacetylase (KDAC) inhibitor to suppress inflammation in peripheral regulatory T (Treg) cells<sup>3,10-12</sup>, neutrophils<sup>13</sup>, macrophages<sup>14</sup> and dendritic cells (DCs)<sup>7</sup>, as well as to prime an antimicrobial program in macrophages<sup>15</sup>. *Clostridia* cluster IV, XIVa, XVIII production of butyrate is also implicated peroxisome proliferator-activated receptor  $\gamma$  (PPAR $\gamma$ ) signaling to limit the lumen oxygen availability and prevent the expansion of *S. Typhimurium* in the intestinal lumen<sup>16,17</sup>.

Beyond modulating host signaling pathways to fortify intestinal barrier integrity and suppress inflammation, microbiota-derived butyrate can also function as a nutrient source and directly attenuate the virulence of enteric pathogens. Depletion of microbiota with broad spectrum antibiotics or streptomycin alone increases host susceptibility to *S. Typhimurium* infection<sup>17</sup>, which can be ameliorated by recolonization with butyrate-producing *Clostridia*<sup>17</sup>. Butyrate production by the microbiota has also been suggested to act as a carbon source for *S. Typhimurium* that expresses the *ydiQRSTD* operon<sup>18</sup>. Notably, butyrate also inhibits the expression of virulence-associated genes in *Salmonella* pathogenicity island-1 (SPI-1) locus<sup>19,20</sup>, which encodes transcriptional regulators, chaperones, secreted protein effectors and needle components of the type III secretion system (T3SS) required for invasion of epithelial cells and bacterial pathogenesis *in vivo*<sup>21</sup>. Nonetheless, the molecular mechanism by which butyrate directly inhibits the expression of SPI-1 virulence genes and *S. Typhimurium* infection is unclear.

To identify the protein targets of butyrate in *S. Typhimurium*, we employed a SCFA chemical reporter and label-free quantitative proteomics. We discovered that several virulence factors encoded within the SPI-1 locus could be acylated in *S. Typhimurium*. Amongst these acylated proteins, we focused on HilA, a key transcriptional regulator of SPI-1 gene expression and *S. Typhimurium* virulence. To address the potential site-specific functions of HilA acylation, we utilized CRISPR-Cas9 gene editing and genetic code expansion to install stable butyryl-lysine analogs at key lysine residues on chromosomally-expressed HilA. Our analysis of these engineered *S. Typhimurium* strains demonstrated that site-specifically butyrylation can inhibit and enhance HilA activity. Notably, acylation of lysine 90 impairs HilA occupancy and expression of SPI-1 genes as well as attenuates *S. Typhimurium* invasion of epithelial cells and pathogenesis *in vivo*. Moreover, a multi-site lysine-to-arginine and acylation-defective HilA mutant strain of *S. Typhimurium* was resistant to butyrate-mediated suppression of SPI-1 genes and slightly more virulent in microbiota-sufficient mice *in vivo*. Our results suggest that microbiota-derived SCFA acylation of key virulence factors may attenuate intestinal pathogen infection *in vivo*.

## Results

### Proteomic analysis of acylated proteins in *Salmonella*.

Given that protein acylation is prevalent in bacteria<sup>22</sup>, we explored whether microbiota-derived butyrate could acylate specific *S. Typhimurium* proteins involved in SPI-1 regulation using an alkyne-butyrate analog (alk-3, pentynoate) (Supplementary Fig. 1a)<sup>23</sup> and chemical proteomics (Supplementary Fig. 1b)<sup>24</sup>. Alk-3 behaved similar to butyrate and did not affect

*S. Typhimurium* (strain 14028S) growth at 10 mM (Supplementary Fig. 1c), but inhibited expression of the SPI-1 gene *sipA* (Supplementary Fig. 1d) and *S. Typhimurium* invasion of HeLa cells (Supplementary Fig. 1e). To visualize acylated proteins, the total cell lysates from alk-3 treated *S. Typhimurium* cultures were reacted via bioorthogonal labeling with azide-rhodamine for in-gel fluorescence profiling (Supplementary Fig. 1b), which revealed many alk-3-modified proteins (Supplementary Fig. 1f). To identify these acylated proteins, alk-3-labeled total cell lysates were reacted with azide-biotin, enriched by streptavidin beads and analyzed by label-free quantitative (LFQ) proteomics. From this analysis, 56 proteins were selectively enriched more than 2-fold in alk-3 samples with *P*-values less than 0.05 (Fig. 1a and Supplementary Dataset). Bioinformatic analysis of the alk-3 hits recovered several proteins involved in metabolism as well as a few key effectors and regulators (SipD, SopB, SipA, SipC, SicA and HilA) of *S. Typhimurium* pathogenesis (Fig. 1a, Supplementary Dataset, and Supplementary Table 1). While the SPI-1 transcriptional regulator HilD has been suggested to modulate propionate activity in *S. Typhimurium*<sup>25</sup> and could be regulated by acetylation<sup>26</sup>, it was not labeled by alk-3 in our proteomic dataset (Supplementary Dataset) or when overexpressed (Supplementary Fig. 2a). Of note, HilA, a key transcriptional regulator of SPI-1 genes<sup>27,28</sup>, was one of the most prominent acylated *S. Typhimurium* candidate proteins in the dataset (Fig. 1a and Supplementary Dataset).

HilA is a transcription regulator that regulates the expression of SPI-1 genes encoding T3SS components and substrates<sup>27–31</sup> and also essential for *S. Typhimurium* infection *in vitro*<sup>32</sup> and pathogenesis *in vivo*<sup>33</sup>. HilA protein is predicted to contain an N-terminal DNA-binding domain (DBD) that is homologous to the OmpR/PhoB-family of transcription factors in bacteria<sup>30</sup>, and a tetratricopeptide repeat (TPR) domain towards the C-terminus (Fig. 1b). To characterize HilA acylation, we expressed epitope-tagged HilA-HA-His6 in *S. Typhimurium* and validated labeling with alk-3 (Supplementary Fig. 2b), which was dose-dependent (Fig. 1c), resistant to hydroxylamine treatment (Supplementary Fig. 2c), and insensitive to the overexpression of *S. Typhimurium* acyltransferase YfiQ (Pat) or deacylase enzyme CobB, respectively (Supplementary Fig. 2d and e), suggesting HilA acylation occurs through posttranslational chemical acylation of lysine residues. In addition, deletion of other candidate protein acyltransferase genes (*yfiQ*, *yliaC*, or *yjaB*), homologous to *E. coli* *yliaC* and *yjaB*<sup>34</sup>, in *S. Typhimurium* did not affect alk-3 labeling of HilA (Supplementary Fig. 2f), further suggesting that millimolar levels of exogenous butyrate chemically acylates HilA through high energy acyl-CoA or phosphate intermediates in *S. Typhimurium*.

To characterize HilA acylation, we expressed and purified HilA-HA-His6 from *S. Typhimurium* incubated with 10 mM butyrate to identify sites of acylation. Of the 34 lysine residues in HilA (Supplementary Fig. 3a), we identified 5 lysines (K90, K231, K324, K456, and K533) that were modified with acetate, propionate or butyrate by LC-MS/MS analysis of tryptic peptides (Supplementary Fig. 3b–d and Supplementary Table 2), consistent with previous HilA acetylation studies<sup>35</sup>. Protein structure prediction of HilA by Robetta<sup>36</sup> suggests that all 5 acylated-lysine residues are located at surface-exposed sites for potential chemical acylation and are in predicted DNA-binding (K90) or protein-protein (K231, K324, K456) interaction domains (Fig. 1b). Amongst the five SCFA-modified lysine residues, K90 was the most prominent acylation site when we compared the ratio of acylated and unmodified peptides (Fig. 1d and Supplementary Table 2).

### Site-specific incorporation of acyl-lysine analogs into HilA.

To evaluate site-specific lysine-butyrylation of HilA in *S. Typhimurium in vivo*, we explored genetic code expansion with *N*<sup>ε</sup>-butyryl-lysine analogs (Supplementary Fig. 4a)<sup>37–39</sup>. Expression of wild-type *Methanosarcina mazei* pyrrolysine-tRNA synthetase (*MmPylRS*-WT) and tRNA<sup>Pyl</sup><sub>CUA</sub> in *S. Typhimurium* showed poor incorporation of *N*<sup>ε</sup>-butyryl-lysine (buK) into overexpressed HilA-HA bearing an amber codon at K90 (HilA-K90-TAG-HA) (Supplementary Fig. 4b and c). We then evaluated other PylRS mutants with buK and other analogs for improved incorporation of potential butyryl-lysine mimics (Supplementary Fig. 4b). Analysis of HilA-HA protein levels revealed that *N*<sup>ε</sup>-pent-4-ynyloxy-carbonyl-lysine<sup>40</sup> afforded near wild-type levels of HilA-K90-TAG-HA with *Methanosarcina barkeri* PylRS-ASF mutant (*MbPylRS*-ASF)<sup>40–42</sup> (Supplementary Fig. 4b and c), which also cross-reacted with anti-butyl-lysine antibody (Supplementary Fig. 4c) and was readily detected by bioorthogonal labeling (Supplementary Fig. 4c). We subsequently employed this compound as a lysine butyrylation-mimic (bmK) in *S. Typhimurium*.

To incorporate bmK into chromosomally-expressed HilA, we optimized CRISPR-Cas9 gene editing<sup>43</sup> in *S. Typhimurium* using single strand DNA templates and liquid selection (Supplementary Fig. 5 and 6). Our optimized CRISPR-Cas9 gene editing protocol enabled chromosomal insertion of an HA-tag at the C-terminus of HilA as well as alanine, glutamine and TAG mutants at K90. The specificity of our CRISPR-Cas9 gene editing protocol was confirmed by whole-genome sequencing of HilA-HA and HilA-K90-TAG-HA *S. Typhimurium* strains (Supplementary Table 3). The activity of the HilA-HA, K90A and K90Q (an acetylation mimic) on SPI-1 gene expression was similar to the parent *S. Typhimurium* (strain 14028S) (Fig. 2a). However, HilA-K90-bmK-HA showed significant reduction of SPI-1 gene expression almost to *hilA* levels (Fig. 2a). These differences in SPI-1 gene expression were correlated with *S. Typhimurium* HilA-K90 mutant infection of HeLa cells (Fig. 2b) and not significant in RAW264.7 macrophages (Fig. 2c), which are less dependent on SPI-1 for invasion<sup>44</sup>. These results demonstrate that classical site-directed mutagenesis to canonical amino acids may not reveal how site-specific metabolite-modifications regulate protein function in cells.

### Site-specific acylation of HilA affects *Salmonella* virulence.

We then generated additional *S. Typhimurium* strains with chromosomal amber codon mutants at K231, K324, K456, and K533 in HilA-HA to evaluate site-specific differences in activity. To control for non-specific effects of bmK incorporation into HilA, we also generated amber codon mutants at K57 and K527 that are not acylated based on our MS/MS analysis but could function as controls for protein expression and activity. Importantly, these engineered HilA-HA strains replicated at similar rates to the parent *S. Typhimurium* strain 14028S in liquid culture (Supplementary Fig. 7a) and efficiently incorporated bmK into the HilA-TAG-HA mutants that were readily detected by bioorthogonal labeling and anti-HA immunoblotting (Fig. 2d). To control for genetic code expansion, the HilA-HA *S. Typhimurium* strain (wt) was also transformed with plasmid encoding PylRS and tRNA<sup>CUA</sup> and labeled with the same concentration of bmK for all subsequent experiments. A comparative analysis of HilA mutants showed that full-length HilA-HA expression in amber codon mutants depended on the presence of bmK (Fig. 2d, Supplementary Fig. 7c and

d). BmK-incorporation at K57, K90 and K527 yielded near wild-type levels of full length protein, whereas K231, K324, 456 and K533 amber codon mutants afforded slightly lower amounts of HilA-HA (Supplementary Fig. 7b and d). Nonetheless, the analysis of these *S. Typhimurium* strains demonstrated that HilA-bmK-HA protein levels are not correlated with the levels of SPI-1 secreted proteins (Fig. 2e), suggesting site-specific effects of lysine-butyrylation on HilA function.

We then evaluated the transcriptional activity of site-specifically acylated HilA mutants in *S. Typhimurium*. Quantitative RT-PCR analysis of HilA target genes showed that relative to wt HilA-HA, site-specific incorporation of bmK at K57, K90, K324 and K456 afforded reduced expression of *prgH*, *invF*, *sipA*, *orgB* and *spaO* located in different operons within the SPI-1 locus (Fig. 3a). While K57 is not acylated, it is predicted to be in the DNA-binding interface of HilA (Fig. 1c) and upon bmK incorporation showed significantly reduced expression of HilA target genes (Fig. 3a), serving as a positive control loss-of-function HilA mutant. Interestingly, acylated-K90 within the DNA-binding domain of HilA (Fig. 1c) also showed significantly reduced expression of HilA target genes with bmK incorporation (Fig. 3a). The incorporation of bmK into the TPR domain of HilA at K324 and K456 also impaired the expression of SPI-1 genes (Fig. 3a). Alternatively, bmK incorporation at K231 afforded slightly enhanced expression of HilA target genes compared to wt HilA-HA, bmK at K527 (non-acylated control for bmK incorporation) and K533 (Fig. 3a). While buK did not get incorporated into HilA-TAG-HA mutants as efficiently as bmK (Supplementary Fig. 4b), we observed similar site-specific effects on the expression of SPI-1 genes, albeit at lower levels (Supplementary Fig. 8a).

To investigate the significance of site-specific acylation of HilA on *S. Typhimurium* virulence, we analyzed the invasion of the HeLa epithelial cell line by *S. Typhimurium*. For these experiments, both wild-type and HilA mutant *S. Typhimurium* strains were transformed with PyIRS and tRNA<sup>CUA</sup> expression plasmid, metabolically labeled with bmK, diluted with PBS buffer and used for infection. In comparison with the other lysine residues in HilA-HA, bmK incorporation at K57 (loss-of-function control), K90, K324 and K456 attenuated *S. Typhimurium* infection of HeLa cells, whereas K231 showed enhanced or similar levels of infection compared to wild-type HilA, K527 (neutral control) and K533 bmK-mutants (Fig. 3b). There was no significant differences in infectivity among the bmK-mutants in RAW264.7 macrophages (Fig. 3c), which is less dependent on SPI-1 invasion<sup>44</sup>. These results demonstrate site-specific lysine-butyrylation of HilA modulates *S. Typhimurium* invasion of epithelial cells, consistent with its modulation of HilA-dependent SPI-1 gene expression (Fig. 3a) and secretion of SPI-1 substrates (Fig. 2d).

Since K90 is the most prominent butyrate modification site in HilA (Fig. 1e and Supplementary Table 2) and afforded significantly reduced expression of SPI-1 genes and *S. Typhimurium* infection with bmK incorporation, we focused on this site of HilA modification for additional functional studies. Indeed, HilA butyrylation levels were increased when *S. Typhimurium* was incubated with butyrate (Supplementary Fig. 8b), and K90 site-specific butyrylation was more than doubled (Supplementary Fig. 8c). To investigate site-specific effects of K90-butyrylation, we evaluated HilA occupancy of SPI-1 genes in *S. Typhimurium*. Crosslinking and HA-immunoprecipitation-sequencing

(x-IP-Seq) analysis of HilA-HA *S. Typhimurium* strains showed that HilA-K90-bmK-HA had decreased occupancy on the promoter regions of HilA-target genes (*prgH* and *invF*) compared to wt HilA-HA (Fig. 4a and Supplementary Fig. 9). Further analysis of HilA-HA variants by crosslinking and HA-immunoprecipitation-qPCR (x-IP-qPCR) revealed site-specific effects of bmK-incorporation on HilA-HA DNA binding (Fig. 4b). Indeed, bmK incorporation at K90 and K57 (loss-of-function control) showed markedly less occupancy of *prgH* and *invF* promoters compared to wt HilA and K527 (neutral control) (Fig. 4b). In contrast, bmK incorporation at K324 and K456 had similar HilA-HA occupancy of these SPI-1 locations (Fig. 4b), suggesting that their inhibitory effects may function not through DNA binding but through alternative mechanisms associated with the predicted TPR domain (Fig. 1c and Supplementary Fig. 10). Interestingly, bmK incorporation at K231 enhanced HilA-HA occupancy at *invF* and *prgH* promoter regions (Fig. 4b), consistent with elevated expression of SPI-1 genes (Fig. 3a) and invasion of HeLa cells (Fig. 3b), suggesting butyrylation of this site may promote HilA oligomerization, DNA-binding and/or transcriptional activity. These results demonstrate site-specific modification of acylated-lysine residues directly modulates the function of HilA in *S. Typhimurium*.

### Site-specific acylation of HilA affects *Salmonella* dissemination.

Given that site-specific bmK incorporation into HilA yielded significant differences in *S. Typhimurium* infection *in vitro*, we explored the infectivity of K90 and K231 bmK-mutants *in vivo*. For these studies, we employed the streptomycin-treatment model of *S. Typhimurium* infection in mice<sup>45</sup>, which has been shown to deplete butyrate-producing microbiota<sup>17</sup> and provide a SCFA-deficient environment for evaluating site-specific modification of HilA mutants *in vivo*. Our initial analysis of bmK-labeled HilA-K90-TAG-HA and HilA-K231-TAG-HA *S. Typhimurium* strains showed similar levels of overall pathogenesis upon oral infection of streptomycin-treated mice compared to *hila S. Typhimurium* (Fig. 5a,b), likely due to depletion of bmK and inactivation of full-length HilA protein expression after multiple days *in vivo*. We thus focused on *S. Typhimurium* dissemination into mesenteric lymph nodes (mLN) and liver early (2 days) post-infection to evaluate acute SPI-1-dependent invasion *in vivo*. For these experiments, we orally infected streptomycin-treated mice with bmK-labeled wt and HilA mutant *S. Typhimurium* strains, harvested their mLN and liver and measured colony-forming units (CFUs) by *Salmonella*-selective agar plates. In comparison to wt *S. Typhimurium*, the bmK-labeled HilA-K90 mutant was defective in dissemination from the intestines, similar to *hila*, while the bmK-labeled HilA-K231 mutant was recovered from mLN and liver at similar levels to wt (Fig. 5c). These results are consistent with previous reports of *hila in vivo*<sup>46</sup>, which is more attenuated than mutations in the SPI-1 needle complex alone<sup>47</sup> since HilA also regulates motility and other environmental response elements in *S. Typhimurium*<sup>48</sup>. Moreover, histological analysis of intestinal sections revealed that wt *S. Typhimurium* caused significant inflammation in the mice cecum, whereas the bmK-labeled HilA-K90 mutant had mild to no inflammation in the cecum (Fig. 5d, and Supplementary Fig. 11). These results demonstrate that site-specific butyrylation of K90 on HilA nearly phenocopies *hila* and is sufficient to attenuate *S. Typhimurium* invasion and dissemination *in vivo*.

### Multi-site HilA mutant is resistant to butyrate inhibition.

Since site-specific HilA lysine butyrylation impaired *S. Typhimurium* virulence, we investigated whether these bacterial strains would be resistant to butyrate inhibition. We initially evaluated K90 to alanine and arginine mutants as potential acylation-deficient mutants, but both single-site mutants showed similar sensitivity to butyrate inhibition of invasion in HeLa cells (Supplementary Fig. 12a). Since K324 and K456 could also be acylated (Supplementary Fig. 3 and Supplementary Table 2) and were inhibited by site-specific bmK incorporation (Fig. 3a and b), we hypothesized that butyrylation of K324 and K456 could still inhibit HilA function and *S. Typhimurium* virulence. We thus tested overexpressed multi-site HilA mutants in which K90, K324, and K456 were all mutated to alanine (K90,324,456A) or arginine (K90,324,456R) (Supplementary Fig. 12b). While the HilA-K90,324,456A mutant showed defective SPI-1 secretion activity and was not useful for butyrate inhibition studies (Supplementary Fig. 12b), the HilA-K90,324,456R exhibited similar SPI-1 secretion activity to wt HilA (Supplementary Fig. 12b). We thus generated HilA-K90,324,456R chromosomal mutant strain, and found that it was resistant to butyrate inhibition of SPI-1 gene expression (Fig. 6a) as well as invasion of HeLa cells (Fig. 6b). We thus explored infectivity of HilA-K90,324,456R mutant strain *in vivo*. Infection of microbiota-sufficient mice containing higher levels of butyrate<sup>17</sup> with the HilA-K90,324,456R mutant strain resulted in shorter survival time compared to wt *S. Typhimurium* (Fig. 6c), which was correlated with a more rapid expansion and shedding of *S. Typhimurium* (Fig. 6d). The difference between wt *S. Typhimurium* and the HilA-K90,324,456R mutant strain was dependent on the microbiota, as streptomycin-treated mice had similar survival time and *S. Typhimurium* fecal load when infected with wt or HilA-K90,324,456R mutant strain (Supplementary Fig. 12c and d). These results further demonstrate that acylation of key virulence factors such as HilA by exogenous butyrate may contribute to microbiota attenuation of *S. Typhimurium* infection *in vivo*.

### Discussion

SCFAs are abundant metabolites generated by microbiota-fermentation of dietary polysaccharides, but the molecular mechanisms by which these prominent gut metabolites inhibit enteric pathogen virulence has been unclear. For example, propionate generated by *Bacteroides* is reported to mediate colonization resistance against *S. Typhimurium* and other *Enterobacteriaceae* by disrupting intracellular pH homeostasis<sup>49,50</sup> as well as destabilizing HilD, another SPI-1 transcriptional regulator<sup>25</sup>, suggesting specific mechanisms from different microbiota species and metabolites that may act cooperatively to prevent *S. Typhimurium* infection *in vivo*. Indeed, our analysis of butyrate, associated with other microbiota species, revealed direct acylation of other SPI-1 factors may be another mechanism to attenuate *S. Typhimurium* virulence. The most prominent target from our chemical proteomic studies was HilA, is a key transcriptional regulator of SPI-1 genes required for *S. Typhimurium* invasion of intestinal epithelial cells and dissemination *in vivo*. To functionally evaluate site-specific HilA butyrylation, we installed butyryl-Lys analogs into chromosomally expressed HilA mutants using CRISPR-Cas9 gene editing and non-canonical amino acid mutagenesis. These constitutively butyryl-Lys-modified HilA mutants revealed site-specific effects on *S. Typhimurium* virulence gene expression, invasion

of epithelial cells and dissemination *in vivo* (Supplementary Fig. 13a). Abrogation of acylation on critical lysine residues on HilA results in resistance to butyrate inhibition *in vitro* and *in vivo*. While HilA acylation is substoichiometric, it can be increased by the millimolar levels of exogenous butyrate reported in the gut and may be further regulated by specific microbiota-butyrate producers *in vivo*. *S. Typhimurium* may therefore sense high concentrations of this SCFA through HilA-acylation to limit invasion of host cells and utilize butyrate as a nutrient source from the microbiota in the intestinal lumen (Supplementary Fig. 13b). Finally, our discovery of inhibitory acylation on specific proteins and amino acid residues suggests repurposing covalent protein modification agents may afford new anti-infectives for SCFA-sensitive pathogens.

## Methods

### Microbial Strains and Growth Conditions.

All strains used are listed in Supplementary Table 4. All *Salmonella* Typhimurium strains used were derivatives of *S. Typhimurium* 14028S<sup>25</sup>. *Salmonella* strains were cultured at 37°C in liquid Miller Luria-Bertani (LB) medium [10 g/L tryptone, 5 g/L yeast extract, 10 g/L NaCl] (Becton Dickinson, Difco™), SPI-1 inducing LB medium [10 g/L tryptone, 5 g/L yeast extract, 300 mM NaCl], or on *Salmonella Shigella* agar (Becton Dickinson). Cultures were grown at 37°C in Multitron shaking incubator (INFORS HT) at 220 rpm. When required, antibiotics were added to the medium as follows: carbenicillin 100 µg/mL, kanamycin 50 µg/mL, and chloramphenicol 10 µg/mL.

### Animal Experiments.

C57BL/6J (000664) mice were purchased from the Jackson Laboratory and maintained at the Rockefeller University animal facilities under SPF conditions. Animal care and experimentation were consistent with the National Institutes of Health guidelines and approved by the Institutional Animal Care and Use Committee of the Rockefeller University.

### Chemicals.

Sodium butyrate was purchased from Sigma-Aldrich (303410). Alk-3 (4-pentynoic acid) was purchased from Sigma-Aldrich (232211). Az-Rho was synthesized in the lab as previously described<sup>51</sup>. Az-biotin was purchased from Sigma-Aldrich (762024). Butyryl-lysine was synthesized according to previously described<sup>38</sup>. BmK was synthesized according to previously described<sup>40</sup>.

### Generation of HilA-K90bu site-specific antibody.

HilA-K90bu peptide (CRILSED(butyrylK)EHRYIE) and HilA-K90 peptide (CRILSEDKEHRYIE) was synthesized in The Rockefeller University Proteomics Resource Center. HilA-K90bu peptide was sent to Thermo Fisher for custom antibody production with a 70-day rabbit immunization protocol. Serum was collected on Day 35, 56 and 58 and measured for titer with ELISA. Site-specific polyclonal antibodies were affinity purified and counter-selected with HilA-K90 peptide.

### **Salmonella growth curve.**

Overnight cultures of *Salmonella* strains in Miller LB were diluted 1:100 to 5 mL fresh SPI-1 inducing LB medium in Falcon round-bottom 15 mL tubes. Cultures were taken out aliquots of 750  $\mu$ L from 0 hour to 5 hours at 1-hour interval. Aliquots were added to 10 mm polystyrene cuvettes (Sarstedt) and OD<sub>600</sub> was measured with Biophotometer plus (Eppendorf).

### **Preparation of *Salmonella* bacterial total cell lysates.**

One to fifty dilutions of overnight Miller LB cultures of *Salmonella* Typhimurium strain 14028s WT overnight culture were grown in 4 mL SPI-1 inducing LB for 4 h at 37°C with 220 rpm shaking. For alk-3 labeling experiments, cultures were incubated with or without 10 mM fresh alk-3 (in dH<sub>2</sub>O). For incorporation of ncAA into overexpressed HilA, cultures were added with 1 mM ncAA and 0.2% arabinose. For incorporation of ncAA into endogenous HilA, cultures were added with 100  $\mu$ M ncAA and 0.01% arabinose. *S.* Typhimurium cells were pelleted at 15000 g for 1 min, and pellets were lysed with 200  $\mu$ L lysis buffer (phosphate-buffered saline (PBS) containing 0.5% Nonidet P-40, 1X EDTA-free protease inhibitor cocktail (Roche), 0.5 mg/mL lysozyme (in dH<sub>2</sub>O) (Sigma), and 1:1,000 dilution of Benzonase (Millipore)). After re-suspension, pellets were sonicated for 10 sec for 3 times, then were incubated on ice for 30 min. Cell lysates were centrifuged at 15000 g for 1 min to remove cell debris and supernatants were collected. Protein concentration was estimated by BCA assay with BCA Protein Assay Kit (Thermo).

### **Salmonella protein immunoprecipitation and immunoblotting.**

From *Salmonella* total cell lysates prepared as described above, protein samples were boiled with 1X Laemmli buffer 95°C for 5 min. 20  $\mu$ L of each sample was loaded onto a 4–20% Tris-HCl gel (Bio-Rad) for SDS-PAGE. Proteins were transferred onto 0.45  $\mu$ m nitrocellulose membrane (Bio-Rad) with Trans-Blot Turbo Transfer System (Bio-Rad) at 25 V for 30 min. Membrane was blocked with 5% non-fat milk in PBS with 0.1% Tween-20 (PBS-T) for 30 min, and primary antibody was added to solution before incubating membrane at 4°C overnight. Dilution of primary antibodies were as follows: for HA-tagged proteins, 1:2,000 anti-HA rabbit antibody H6908 (Sigma); for FLAG-tagged proteins, 1:2000 anti-FLAG rabbit antibody F7425 (Sigma); for HilA-K90Bu antigen, 1:200 anti-HilAK90Bu rabbit custom antibody (Thermo Fisher) or 1:200 anti-HilAK90 rabbit custom antibody (Thermo Fisher). Membrane was washed with PBS-T 3 times, and incubated with 1:10,000 goat polyclonal anti-rabbit HRP ab97051 (Abcam) in PBS-T with 5% non-fat milk at room temperature for 1 hour. Membrane was washed with PBS-T 3 times, and imaged with Clarity Western ECL substrate (Bio-Rad) and ChemiDoc XRS+ System (Bio-Rad).

For *Salmonella* protein immunoprecipitation, 250  $\mu$ g of each total cell lysates were incubated with 20  $\mu$ L PBS-T-washed EZview™ Red Anti-HA Affinity Gel (Sigma) at 4 °C for 1 hour with end-to-end rotation. Samples were washed with 200  $\mu$ L PBS-T for 3 times, before being boiled with 1X Laemmli buffer 95°C for 5 min. 20  $\mu$ L of each sample was loaded onto a 4–20% Tris-HCl gel (Bio-Rad) for SDS-PAGE and further immunoblotting.

### In-gel fluorescence analysis of alk-3 labeling.

For in-gel fluorescence analysis of alk-3 labeled *Salmonella* proteome, from the alk-3-treated or control total cell lysates prepared as described above, 45  $\mu$ L of each total cell lysates (~50  $\mu$ g) was added with 5  $\mu$ L of click chemistry reagents as a 10X master mix (az-Rho: 0.1 mM, 10 mM stock solution in DMSO; tris(2-carboxyethyl)phosphine hydrochloride (TCEP): 1 mM, 50 mM freshly prepared stock solution in dH<sub>2</sub>O; tris[(1-benzyl-1H-1,2,3-triazol-4-yl)methyl]amine (TBTA): (0.1 mM, 2 mM stock in 4:1 t-butanol:DMSO); CuSO<sub>4</sub> (1 mM, 50 mM freshly prepared stock in dH<sub>2</sub>O). Samples were mixed well and incubated at room temperature for 1 h. After incubation, samples were mixed with 200  $\mu$ L cold methanol, 150  $\mu$ L cold water, and 75  $\mu$ L cold chloroform. Sample proteins were precipitated at 18000 g for 1 min at 4 °C. After gently removing the aqueous layer, protein pellets were washed with 200  $\mu$ L cold methanol, spinning down at 18000 g for 1 min at 4 °C, and liquid was gently decanted. After washing twice, pellets were allowed air-dried before boiling with 1X Laemmli buffer.

For in-gel fluorescence analysis of alk-3 labeled H1A, from the alk-3-treated or control total cell lysates prepared as described above, 250  $\mu$ g of each total cell lysates were immunoprecipitated with 20  $\mu$ L PBS-T-washed EZview™ Red Anti-HA Affinity Gel (Sigma). After samples were washed with 200  $\mu$ L PBS-T for 3 times, 36  $\mu$ L of PBS was added to each sample. 4  $\mu$ L of click chemistry reagents as a 10X master mix mentioned above were added to each sample. Samples were mixed well and incubated at room temperature for 1 h. After incubation, samples were washed with 200  $\mu$ L PBS-T for 3 times.

Samples were boiled with 1X Laemmli buffer 95°C for 5 min before being loaded onto a 4–20% Tris-HCl gel (Bio-Rad) for SDS-PAGE. In-gel fluorescence scanning was performed using a Typhoon 9400 imager (Amersham Biosciences).

### Alk-3 labeling Label-Free Quantitative proteomics.

One to fifty dilutions of overnight Miller LB cultures of *Salmonella* Typhimurium strain 14028s WT overnight culture were grown in 20 mL SPI-1 inducing LB for 4 h at 37°C with 220rpm shaking, each sample growing in 4 mL aliquots. Cultures were incubated with or without 10 mM fresh alk-3 (in dH<sub>2</sub>O). Cultures were pooled back to 20 mL per sample in Falcon tubes, and lysed in lysis buffer described above. After re-suspension in 1 mL lysis buffer, bacteria were sonicated for 15 sec with Sonic Dismembrator Model 500 (Fisher Scientific) with 5 sec on and 10 sec off per cycle. Cell lysates were centrifuged at 15000 g for 1 min to remove cell debris and supernatants were collected. Each total cell lysates (~2 mg) was added with 100  $\mu$ L of click chemistry reagents as a 10X master mix (az-Biotin: 0.1 mM, 10 mM stock solution in DMSO; tris(2-carboxyethyl)phosphine hydrochloride (TCEP): 1 mM, 50 mM freshly prepared stock solution in dH<sub>2</sub>O; tris[(1-benzyl-1H-1,2,3-triazol-4-yl)methyl]amine (TBTA): (0.1 mM, 2 mM stock in 4:1 t-butanol:DMSO); CuSO<sub>4</sub> (1 mM, 50 mM freshly prepared stock in dH<sub>2</sub>O). Samples were mixed well and incubated at room temperature for 1 h. After incubation, samples were mixed with 4 mL cold methanol and incubated at –20°C overnight. Protein pellets were centrifuged at 5000 g for 30 min at 4°C, and were washed with 1 mL cold methanol 3 times. After last wash, pellets were let

air dried before being re-solubilized in 250  $\mu$ L 4% SDS PBS with bath sonication. Solutions were diluted with 750  $\mu$ L PBS, and incubated with 60  $\mu$ L PBS-T-washed High Capacity NeutrAvidin agarose (Pierce) at room temperature for 1 h with end-to-end rotation. Agarose were washed with 500  $\mu$ L 1% SDS PBS 3 times, 500  $\mu$ L 2M Urea PBS 3 times, and 500  $\mu$ L PBS 3 times. Agarose were then reduced with 100  $\mu$ L 10 mM DTT (Sigma) in PBS for 30 min at 37°C, and alkylated with 100  $\mu$ L 50 mM iodoacetamide (Sigma) in PBS for 20 min in dark. On-bead proteins were digested with 400 ng Trypsin/Lys-C mix (Promega) at 37°C overnight with shaking. Digested peptides were collected and lyophilized before being desalted with custom-made stage-tip containing Empore SPE Extraction Disk (3M). Peptides were eluted with 2% acetonitrile, 2% formic acid in dH<sub>2</sub>O.

Peptide LC-MS analysis was performed as described previously<sup>52</sup>. Briefly, samples were analyzed with a Dionex 3000 nano-HPLC coupled to an Orbitrap XL mass spectrometer (Thermo Fisher). Peptide samples were pressure-loaded onto a home-made C18 reverse-phase column (75  $\mu$ m diameter, 15 cm length). A 180-minute gradient from 95% buffer A (HPLC grade water with 0.1% formic acid) and 5% buffer B (HPLC grade acetonitrile with 0.1% formic acid), to 25% buffer A and 75% buffer B in 133 minutes was used at 200 nL/min. The Orbitrap XL was operated in top-8-CID-mode with MS spectra measured at a resolution of 60,000@m/z 400. One full MS scan (300–2000 MW) was followed by three data-dependent scans of the *n*th most intense ions with dynamic exclusion enabled. Peptides fulfilling a Percolator-calculated 1% false discovery rate (FDR) threshold were reported.

Label-free quantification of alk-3 labeled proteins was performed with the label-free MaxLFQ algorithm in MaxQuant software as described<sup>53</sup>. The search results from MaxQuant were analyzed by Perseus (<http://www.perseusframework.org/>). Briefly, the control replicates and alk-3 labeled sample replicates were grouped correspondingly. The results were cleaned to filter off reverse hits and contaminants. Only proteins that were identified in all alk-3 labeled sample replicates and with more than two unique peptides were subjected to subsequent statistical analysis. LFQ intensities were used for measuring protein abundance and logarithmized. Signals that were originally zero were imputed with random numbers from a normal distribution, whose mean and standard deviation were chosen to best simulate low abundance values below the noise level (Replace missing values by normal distribution with Width = 0.3 and Shift = 2.2). Significant proteins enriched in alk-3 labeled sample group versus control group were determined by a threshold strategy, in which ratio larger than or equals to 2 and *P*-value smaller than 0.05 were categorized as hits. The resulting table was exported as Supplementary Dataset.

### MS/MS detection of protein PTM.

One to fifty dilutions of overnight Miller LB cultures of *Salmonella* Typhimurium strain 14028s *hilA* pBAD-HilA-HA-His overnight culture were grown in 500 mL SPI-1 inducing LB with 10 mM sodium propionate or 10 mM sodium butyrate for 2 h at 37°C with 220rpm shaking, before 0.2% arabinose was added to induce HilA-HA-His expression for 3 h. Bacteria was harvested with 5000 g for 10 min at 4°C, and lysed in 25 mL lysis buffer described above with 1 mM EDTA and 50 mM nicotinamide (NAM). bacteria were sonicated for 5 min with Sonic Dismembrator Model 500 (Fisher Scientific) with 5 sec

on and 10 sec off per cycle. Lysates were centrifuged at 5000 g for 10 min at 4°C, and supernatants were filtered with 0.22 µm filter before being loaded onto HisTrap FF 5mL column (GE Healthcare). HilA-HA-His protein was purified with wash with 3 Column Volume (CV) 100% buffer A (PBS-T, 50 mM NAM), wash with 5 CV 10% buffer B (PBS-T, 50 mM NAM, 300 mM imidazole), and 5 CV elution with gradient from 10% to 100% buffer B. Fractions containing HilA was pooled and dialyzed to PBS-T with 3 spin-dilution cycles in 10,000 MWCO filter (Amicon). Purified HilA-HA-His was immunoprecipitated with anti-butyrilysine antibody (PTM Biolab)- or anti-propionyllysine antibody (PTM Biolab)-conjugated protein A/G magnetic beads (Pierce), and samples were boiled and run on SDS-PAGE. Coomassie Blue-stained bands corresponding to HilA was cut out, reduced with 10 mM DTT (Sigma) in fresh 100 mM ammonium bicarbonate (ABC) for 30 min at 37°C, and alkylated with 50 mM iodoacetamide (Sigma) in fresh 100 mM ABC for 20 min in dark. Gel pieces were digested with 200 ng Trypsin/Lys-C mix (Promega) at 37°C overnight with shaking.

### ***Salmonella* CRISPR-Cas9 genome editing.**

To make electrocompetent *Salmonella* Typhimurium, overnight culture of *Salmonella* Typhimurium strains were diluted 1:50 to 100 mL fresh LB, and were grown at 37°C in shaking incubator at 220 rpm for 2 hours, until OD<sub>600</sub> reached 0.5 to 0.7. Cells were pelleted at 5000 g for 10 min at 4°C, and washed with 50 mL ice-cold 10% glycerol twice. Cell pellets were resuspended in 500 µL 10% glycerol, and aliquoted 50 µL per tube. Electrocompetent parent *Salmonella* Typhimurium strains were transformed with pKD46 via electroporation with Gene Pulser II (Bio-Rad) at 2.5 kV and 25 µF in 2 mm cuvette, and selected on Ampicillin agar plates at 30 °C overnight. The resulting *Salmonella* Typhimurium pKD46 strains were made into electrocompetent cells after grown at 30°C with 0.2% arabinose and ampicillin. *Salmonella* Typhimurium pKD46 electrocompetent cells were transformed with 2 µL pWJ297-sgRNA (~100 ng) and 10 µL 10 uM ssDNA editing template and selected on Chloramphenicol agar plates at 37 °C overnight. All colonies on the plate were collected with cell scraper and resuspended in 4 mL LB with Chloramphenicol. The bacterial suspension were diluted 1:50 to 4 mL fresh LB with Chloramphenicol, and were grown at 37°C in Multitron shaking incubator (INFORS HT) at 220 rpm for 2 hours. Culture was streaked onto Chloramphenicol agar plates, and colonies from the plates were randomly picked for colony PCR to confirm successful editing. Successfully edited colonies were streaked onto plain agar plates to cure pWJ297-sgRNA, and curing was confirmed by streaking on Chloramphenicol agar plates.

Optimization of *Salmonella* CRISPR-Cas9 genome editing are described as follows. The protocol for CRISPR-Cas9 genome editing in *E. coli*<sup>43</sup> resulted in very high false-positive rate and an estimated editing efficiency of less than 5% (data not shown). To increase editing efficiency, we introduced synonymous co-mutation of nearest PAM together with targeted sequence, and used gRNA specific for that PAM to guide Cas9 (Supplementary Fig. 5a). As an example, we set out to mutate Lys90 to Ala in HilA. Synonymous PAM co-mutation (c243g) increased editing efficiency and resulted in successful editing (Supplementary Fig. 5b). Colonies selected for pWJ297 (pCas9) and pCRISPR were mostly false-positive, meaning that CRISPR-Cas9 system did not impose an adequate selection pressure. We



total inputs. 750  $\mu$ L of the remaining supernatants of each were incubated with 2  $\mu$ L anti-HA ChIP-grade polyclonal antibody (ab91110, Abcam) at 4°C for 1 h with end-to-end rotation. The solutions were then added to 30  $\mu$ L PBS-T-washed protein A/G magnetic beads (Pierce) and incubated at 4°C for 1 h with end-to-end rotation. Beads were washed with 500  $\mu$ L 1X RIPA buffer twice, 500  $\mu$ L LiCl Wash buffer (10 mM Tris-HCl, pH 8.0, 250 mM LiCl, 1 mM EDTA, 0.5% NP-40, 0.5% sodium deoxycholate) twice, and 500  $\mu$ L Tris-EDTA buffer (10 mM Tris-HCl, pH 8.0, 1 mM EDTA) once. Samples were eluted with 100  $\mu$ L SDS Elution buffer (50 mM Tris-HCl, pH 8.0, 10 mM EDTA, 1% SDS) at 65°C for 10 min. Each total input sample and ChIP sample were added with 5  $\mu$ L 20 mg/mL proteinase K (Qiagen) and de-crosslinked at 65°C overnight. All de-crosslinked samples were purified with E.Z.N.A. Cycle Pure kit (Omega Bio-tek) and eluted with 100  $\mu$ L elution buffer in the kit. ChIP-qPCR were performed with PowerUp SYBR Green Master Mix (Applied Biosystems) per manufacturer's manual and primers listed in Supplementary Table 5. Same samples were sent to Rockefeller University Genomics Center for library preparation and sequenced with NextSeq High Output 75 Single-Read sequencing.

### ***In vitro* invasion assay and intracellular survival assay.**

HeLa cells were cultured in 12-well tissue culture plates at 80–90% confluency. Wells were added with *Salmonella* cells at an MOI = 10:1 and centrifuged at 1000 g for 5 min. Cells were incubated at 37°C with 5% CO<sub>2</sub> for 30 min to allow invasion. The media was then replaced with medium containing 100  $\mu$ g/mL gentamicin and incubated for an additional hour to kill extracellular *Salmonella*. Wells were then washed 3 times with PBS, and cells were lysed with 500  $\mu$ L 1% Triton X-100 PBS. Lysates were serially diluted and drip-dropped on *Salmonella Shigella* agar plates (BD 211597) to determine the number of invaded bacteria.

For intracellular survival assay of *Salmonella*, after incubation with medium containing 100  $\mu$ g/mL gentamicin for 1 h, media was replaced with medium containing 10  $\mu$ g/mL gentamicin and incubated for additional 4.5 hours at 37°C, 5% CO<sub>2</sub>. Intracellular bacterial counts were obtained by lysing cells and drip-dropping serial dilutions on *Salmonella Shigella* agar plates.

### **S. Typhimurium infection of mice.**

For streptomycin treatment experiments, C57BL/6J SPF mice were gavaged with a single dose of 20 mg of streptomycin 24 hours before infection. Bacterial cultures of different *S. Typhimurium* strains were washed and re-suspended in sterile phosphate-buffered saline (PBS) at 10<sup>7</sup> CFU/mL. Mice were gavaged with 100  $\mu$ L of the bacterial suspension (10<sup>6</sup> CFU). Leftover inocula were serially diluted and plated to confirm the number of CFU administered.

For 48 h infection experiments, mice were euthanized 48 hours after *S. Typhimurium* gavage. Colony-forming units (CFU) in the livers and mesenteric lymph nodes (mLN) were determined by plating five serial dilutions of livers or mLN suspended in sterile 0.1% Triton X-100 PBS on *Salmonella Shigella* agar (BD 211597). Resulting quantities were normalized to liver or mLN weight.

For *S. Typhimurium* infection survival assay, mice weight loss was monitored starting just before infection, and mice were euthanized when they reached 80% baseline weight, appeared hunched or moribund, or exhibited a visibly distended abdomen (indicative of peritoneal effusion), whichever occurred first. Death was not used as an end point.

### Quantification and Statistical Analysis.

Comparisons and statistical tests were performed as indicated in each figure legend. Briefly, Pairwise comparisons were generated with two-tailed t tests. For comparisons of multiple groups over time or with two variables, a two-way analysis of variance (ANOVA) was used with an appropriate Bonferroni posttest comparing all groups to each other, all groups to a control, or selected groups to each other. Survival data were analyzed using a log-rank (Mantel-Cox) test with a Bonferroni correction for the degrees of freedom based on the number of comparisons made. To compare two groups with non-normal distribution or low sample size, the medians of the two groups were compared using a Mann-Whitney test, unless one data set contained only zero values. In these cases, a Mann-Whitney test could not be performed because all values in the group were identical; a Wilcoxon test was performed instead. For comparisons of multiple groups with only one variable, a one-way ANOVA or Kruskal-Wallis test was performed for data with underlying normal or non-normal distribution, respectively, with Bonferroni, Dunnett's, or Dunn's posttests where appropriate. Statistical analyses were performed in GraphPad Prism software. A *P* value of less than 0.05 was considered significant, denoted as \**P* 0.05, \*\**P* 0.01, and \*\*\**P* 0.001 for all analyses.

### Data and materials availability

The data and materials that support the findings of this study are available from the corresponding author upon reasonable request.

### Supplementary Material

Refer to Web version on PubMed Central for supplementary material.

### Acknowledgments:

We thank Milica Tesic Mark, Henry Zebroski and Henrik Molina at The Rockefeller Proteomics Resource Center for liquid chromatography-mass spectrometry analyses and butyrylated peptide synthesis. We thank Weill Cornell School of Medicine Electron Microscopy and Histology Core and Memorial Sloan-Kettering Cancer Center Pathology Core for assistance to histology sample preparation and scoring. We thank Shixian Lin and Peng Chen (Peking University) for *Salmonella* amber codon expression plasmids, Wenyan Jiang and Luciano Marraffini (Rockefeller University) for bacterial CRISPR-Cas9 plasmids, Helene Andrews-Polymeris (Texas A&M College of Medicine) and Michael McClelland (University of California, Irvine) for *S. Typhimurium hilA* strain from NIAID, NIH: *Salmonella enterica* subsp. *enterica*, Strain 14028s (Serovar Typhimurium) Single-Gene Deletion Mutant Library, James Slauch (University of Illinois at Urbana-Champaign) for *S. Typhimurium tetRA-hilD-3xFlag* strain, Chien-Che Hung and Craig Altier (Cornell University) for providing *S. Typhimurium* strain 14028S and helpful discussions and Jorge Galan (Yale University) for helpful discussions. Z.J.Z. received support from the David Rockefeller Graduate Program. H.C.H. acknowledges support from NIH grants (R01GM087544 and R01AT007671) and Lerner Trust.

## References:

1. Rooks MG & Garrett WS Gut microbiota, metabolites and host immunity. *Nature Reviews Immunology* 16, 341–352 (2016).
2. Cummings JH, Pomare EW, Branch WJ, Naylor CP & Macfarlane GT Short chain fatty acids in human large intestine, portal, hepatic and venous blood. *Gut* 28, 1221–1227 (1987). [PubMed: 3678950]
3. Atarashi Ket al. Induction of colonic regulatory T cells by indigenous *Clostridium* species. *Science* (80-. ). 331, 337–41 (2011).
4. Donohoe DRet al. The microbiome and butyrate regulate energy metabolism and autophagy in the mammalian colon. *Cell Metab.* 13, 517–526 (2011). [PubMed: 21531334]
5. Elinav Eet al. NLRP6 inflammasome regulates colonic microbial ecology and risk for colitis. *Cell* 145, 745–757 (2011). [PubMed: 21565393]
6. Voltolini Cet al. A novel antiinflammatory role for the short-chain fatty acids in human labor. *Endocrinology* 153, 395–403 (2012). [PubMed: 22186417]
7. Trompette Aet al. Gut microbiota metabolism of dietary fiber influences allergic airway disease and hematopoiesis. *Nat. Med* 20, 159–166 (2014). [PubMed: 24390308]
8. Singh Net al. Activation of Gpr109a, receptor for niacin and the commensal metabolite butyrate, suppresses colonic inflammation and carcinogenesis. *Immunity* 40, 128–139 (2014). [PubMed: 24412617]
9. Macia Let al. Metabolite-sensing receptors GPR43 and GPR109A facilitate dietary fibre-induced gut homeostasis through regulation of the inflammasome. *Nat. Commun* 6, 6734 (2015). [PubMed: 25828455]
10. Furusawa Yet al. Commensal microbe-derived butyrate induces the differentiation of colonic regulatory T cells. *Nature* 504, 446–50 (2013). [PubMed: 24226770]
11. Arpaia Net al. Metabolites produced by commensal bacteria promote peripheral regulatory T-cell generation. *Nature* 504, 451–455 (2013). [PubMed: 24226773]
12. Smith PMet al. The Microbial Metabolites, Short-Chain Fatty Acids, Regulate Colonic Treg Cell Homeostasis. *Science* (80-. ). 341, 569–573 (2013).
13. Vinolo MAREt al. Suppressive effect of short-chain fatty acids on production of proinflammatory mediators by neutrophils. *J. Nutr. Biochem* 22, 849–855 (2011). [PubMed: 21167700]
14. Chang PV, Hao L, Offermanns S & Medzhitov R The microbial metabolite butyrate regulates intestinal macrophage function via histone deacetylase inhibition. *Proc. Natl. Acad. Sci* 111, 2247–2252 (2014). [PubMed: 24390544]
15. Schulthess Jet al. The Short Chain Fatty Acid Butyrate Imprints an Antimicrobial Program in Macrophages. *Immunity* 50, 432–445.e7 (2019). [PubMed: 30683619]
16. Byndloss MXet al. Microbiota-activated PPAR- $\gamma$  signaling inhibits dysbiotic Enterobacteriaceae expansion. *Science* (80-. ). 357, 570–575 (2017).
17. Rivera-Chávez Fet al. Depletion of Butyrate-Producing Clostridia from the Gut Microbiota Drives an Aerobic Luminal Expansion of Salmonella. *Cell Host Microbe* 19, 443–454 (2016). [PubMed: 27078066]
18. Bronner DNet al. Genetic Ablation of Butyrate Utilization Attenuates Gastrointestinal Salmonella Disease. *Cell Host Microbe* 23, 266–273.e4 (2018). [PubMed: 29447698]
19. Gantois Iet al. Butyrate specifically down-regulates Salmonella pathogenicity island 1 gene expression. *Appl. Environ. Microbiol* 72, 946–949 (2006). [PubMed: 16391141]
20. Lawhon SD, Maurer R, Suyemoto M & Altier C Intestinal short-chain fatty acids alter Salmonella typhimurium invasion gene expression and virulence through BarA/SirA. *Mol. Microbiol* 46, 1451–1464 (2002). [PubMed: 12453229]
21. Groisman E. a & Ochman H Cognate gene clusters govern invasion of host epithelial cells by Salmonella typhimurium and Shigella flexneri. *EMBO J.* 12, 3779–3787 (1993). [PubMed: 8404849]

22. Hentchel KL & Escalante-Semerena JC Acylation of Biomolecules in Prokaryotes: a Widespread Strategy for the Control of Biological Function and Metabolic Stress. *Microbiol. Mol. Biol. Rev* 79, 321–346 (2015). [PubMed: 26179745]
23. Yang Y-Y, Ascano JM & Hang HC Bioorthogonal chemical reporters for monitoring protein acetylation. *J. Am. Chem. Soc* 132, 3640–3641 (2010). [PubMed: 20192265]
24. Grammel M & Hang HC Chemical reporters for biological discovery. *Nature Chemical Biology* 9, 475–84 (2013). [PubMed: 23868317]
25. Hung C-CC et al. The intestinal fatty acid propionate inhibits *Salmonella* invasion through the post-translational control of HilD. *Mol. Microbiol* 87, 1045–1060 (2013). [PubMed: 23289537]
26. Sang Yet et al. Acetylation Regulating Protein Stability and DNA-Binding Ability of HilD, thus Modulating *Salmonella* Typhimurium Virulence. *J. Infect. Dis* 216, 1018–1026 (2017). [PubMed: 28329249]
27. Lostroh CP, Bajaj V & Lee CA The cis requirements for transcriptional activation by HilA, a virulence determinant encoded on SPI-1. *Mol. Microbiol* 37, 300–315 (2000). [PubMed: 10931326]
28. Bajaj V, Lucas RL, Hwang C & Lee CA Co-ordinate regulation of *Salmonella* typhimurium invasion genes by environmental and regulatory factors is mediated by control of hilA expression. *Mol. Microbiol* 22, 703–714 (1996). [PubMed: 8951817]
29. Ellermeier JR & Slauch JM Adaptation to the host environment: regulation of the SPI1 type III secretion system in *Salmonella enterica* serovar Typhimurium. *Curr. Opin. Microbiol* 10, 24–9 (2007). [PubMed: 17208038]
30. Bajaj V, Hwang C & Lee CA hilA is a novel ompR/toxR family member that activates the expression of *Salmonella* typhimurium invasion genes. *Mol. Microbiol* 18, 715–727 (1995). [PubMed: 8817493]
31. Lostroh CP & Lee CA The HilA box and sequences outside it determine the magnitude of HilA-dependent activation of P(prgH) from *Salmonella* pathogenicity island 1. *J. Bacteriol* 183, 4876–85 (2001). [PubMed: 11466291]
32. Eichelberg K & Galan JE Differential Regulation of *Salmonella* typhimurium Type III Secreted Proteins by Pathogenicity Island 1 (SPI-1)-Encoded Transcriptional Activators InvF and HilA. *Infect. Immun* 67, 4099–4105 (1999). [PubMed: 10417179]
33. Boddicker JD, Knosp BM & Jones BD Transcription of the *Salmonella* Invasion Gene Activator, hilA, Requires HilD Activation in the Absence of Negative Regulators. *J. Bacteriol* 185, 525–533 (2003). [PubMed: 12511499]
34. Christensen DG et al. Identification of Novel Protein Lysine Acetyltransferases in *Escherichia coli*. *MBio* 9, e01905–18 (2018).
35. Sturm AB Bistable regulation of *tss-1* genes in *Salmonella* Typhimurium. (Diss., Eidgenössische Technische Hochschule ETH Zürich, Nr. 19635, 2011, 2011). doi:10.3929/ethz-a-006715280
36. Kim DE, Chivian D & Baker D Protein structure prediction and analysis using the Robetta server. *Nucleic Acids Res.* 32, W526–W531 (2004). [PubMed: 15215442]
37. Chin JW Expanding and reprogramming the genetic code. *Nature* 550, 53–60 (2017). [PubMed: 28980641]
38. Gattner MJ, Vrabel M & Carell T Synthesis of  $\epsilon$ -N-propionyl-,  $\epsilon$ -N-butyryl-, and  $\epsilon$ -N-crotonyl-lysine containing histone H3 using the pyrrolysine system. *Chem. Commun. (Camb)* 49, 379–81 (2013). [PubMed: 23192406]
39. Neumann H, Peak-Chew SY & Chin JW Genetically encoding N(epsilon)-acetyllysine in recombinant proteins. *Nat. Chem. Biol* 4, 232–4 (2008). [PubMed: 18278036]
40. Li Jet et al. Ligand-free palladium-mediated site-specific protein labeling inside gram-negative bacterial pathogens. *J. Am. Chem. Soc* 135, 7330–7338 (2013). [PubMed: 23641876]
41. Zhang Met et al. A genetically incorporated crosslinker reveals chaperone cooperation in acid resistance. *Nat. Chem. Biol* 7, 671–677 (2011). [PubMed: 21892184]
42. Lin Set et al. Site-specific incorporation of photo-cross-linker and bioorthogonal amino acids into enteric bacterial pathogens. *J. Am. Chem. Soc* 133, 20581–7 (2011). [PubMed: 22084898]
43. Jiang W, Bikard D, Cox D, Zhang F & Marraffini L. a. RNA-guided editing of bacterial genomes using CRISPR-Cas systems. *Nat. Biotechnol* 31, 233–9 (2013). [PubMed: 23360965]

44. Drecktrah D, Knodler LA, Ireland R & Steele-Mortimer O The mechanism of Salmonella entry determines the vacuolar environment and intracellular gene expression. *Traffic* 7, 39–51 (2006). [PubMed: 16445685]
45. Barthel Met al.Pretreatment of mice with streptomycin provides a Salmonella enterica serovar Typhimurium colitis model that allows analysis of both pathogen and host. *Infect. Immun*71, 2839–2858 (2003). [PubMed: 12704158]
46. Ellermeier CD, Ellermeier JR & Slauch JM HilD, HilC and RtsA constitute a feed forward loop that controls expression of the SPI1 type three secretion system regulator hilA in Salmonella enterica serovar Typhimurium. *Mol. Microbiol* 57, 691–705 (2005). [PubMed: 16045614]
47. Hapfelmeier Set al.The Salmonella Pathogenicity Island (SPI)-2 and SPI-1 Type III Secretion Systems Allow Salmonella Serovar typhimurium to Trigger Colitis via MyD88-Dependent and MyD88-Independent Mechanisms. *J. Immunol*174, 1675–1685 (2005). [PubMed: 15661931]
48. Thijs IMVet al.Delineation of the Salmonella enterica serovar Typhimurium HilA regulon through genome-wide location and transcript analysis. *J. Bacteriol*189, 4587–4596 (2007). [PubMed: 17483226]
49. Jacobson Aet al.A Gut Commensal-Produced Metabolite Mediates Colonization Resistance to Salmonella Infection. *Cell Host Microbe*24, 296–307.e7 (2018). [PubMed: 30057174]
50. Sorbara MTet al.Inhibiting antibiotic-resistant Enterobacteriaceae by microbiota-mediated intracellular acidification. *J. Exp. Med*216, 84–98 (2019). [PubMed: 30563917]

## References

51. Rangan KJ, Yang Y-Y, Charron G & Hang HC Rapid visualization and large-scale profiling of bacterial lipoproteins with chemical reporters. *J. Am. Chem. Soc* 132, 10628–10629 (2010). [PubMed: 20230003]
52. Peng T & Hang HC Bifunctional fatty acid chemical reporter for analyzing S-palmitoylated membrane protein-protein interactions in mammalian cells. *J. Am. Chem. Soc* 137, 556–9 (2015). [PubMed: 25575299]
53. Cox Jet al.Accurate proteome-wide label-free quantification by delayed normalization and maximal peptide ratio extraction, termed MaxLFQ. *Mol. Cell. Proteomics*13, 2513–26 (2014). [PubMed: 24942700]
54. Court DL, Sawitzke J. a & Thomason LC Genetic engineering using homologous recombination. *Annu. Rev. Genet* 36, 361–88 (2002). [PubMed: 12429697]

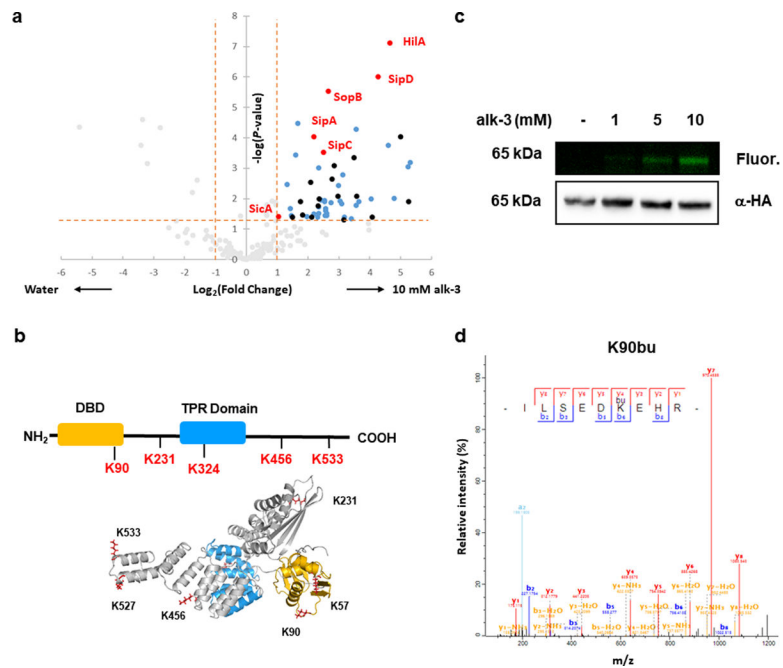


**Figure 1. Proteomic analysis of acylated proteins in *S. Typhimurium*.**

(a) LFQ proteomic analysis of alk-3-labeled proteins in *S. Typhimurium* ( $n = 4$ ). *S. Typhimurium* cell lysates were reacted with az-biotin for the enrichment of alk-3-labeled proteins with streptavidin beads and identification by LC-MS/MS. Proteins that were enriched by alk-3 (top right corner) were colored according to their annotated biological function. Blue, metabolic enzymes. Red, SPI-1 proteins. Black, other proteins. (b) Domain architecture (top) and predicted structure of HilA (bottom). Domain architecture was assigned by NCBI Conserved Domain Search. Structure prediction was performed with Robetta. DBD, DNA-binding domain, yellow. TPR, tetratricopeptide repeat, blue. Lysine residues detected to be acylated (K90, K231, K324, K456, K533) and two additional lysine residues that serve as controls (K57, K527) are highlighted in red. K324 is buried in the back (see Supplementary Fig. 9). (c) Alk-3 dose-dependent labeling on HilA. *S. Typhimurium* *hilA* overexpressing HilA-HA-His were grown with different concentrations of alk-3 before cell lysates were reacted with az-Rho, followed by anti-HA immunoprecipitation, SDS-PAGE in-gel fluorescence scanning (top), and anti-HA immunoblotting (bottom). Also see Supplementary Fig. 14. (d) MS/MS spectrum of HilA K90 butyrylated peptide detected from HilA purified from *S. Typhimurium* grown with 10 mM butyrate.

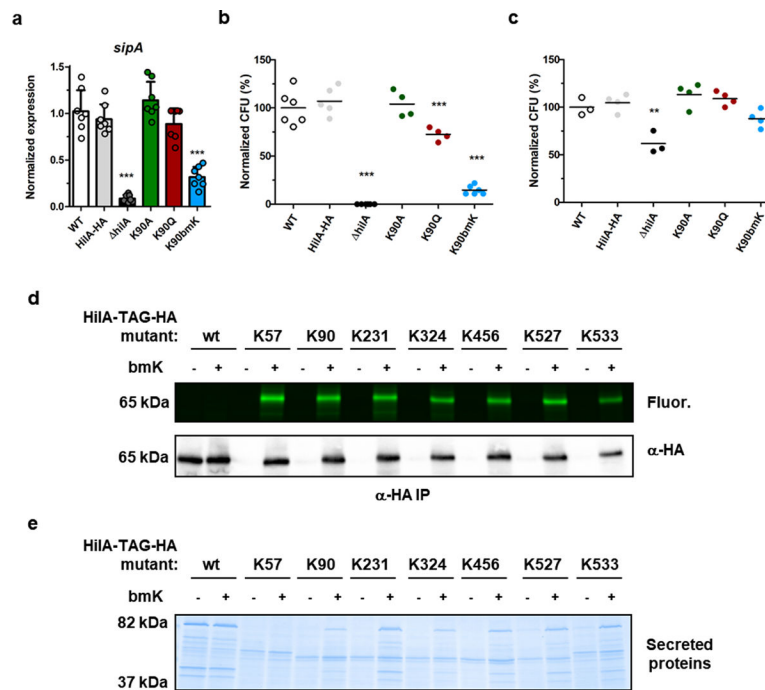


**Figure 2. Site-specific mutation of HilA affects *S. Typhimurium* virulence.**

(a) Relative expression level of SPI-1 gene *sipA* in *S. Typhimurium* WT, HilA-HA strain, *hilA* strain, HilAK90A-HA and HilAK90Q-HA mutants measured by qRT-PCR ( $n = 7-8$ ). All mutants were compared to WT with one-way ANOVA and Dunnett post-test. Error bar, SD. \*\*,  $P$ -value  $< 0.01$ ; \*\*\*,  $P$ -value  $< 0.001$ . Comparisons with no asterisk had  $P$ -value  $> 0.05$  and were not considered significant. (b and c) Gentamicin protection assay of *S. Typhimurium* WT, HilA-HA strain, *hilA* strain, HilAK90A-HA, HilAK90Q-HA, and HilAK90bmK-HA mutants infecting HeLa cells (b) or RAW264.7 macrophages (c) at MOI = 10 ( $n = 3-6$ ). All mutants were compared to HilA-HA with one-way ANOVA and Dunnett post-test. Centerline, average. \*\*,  $P$ -value  $< 0.01$ . Comparisons with no asterisk had  $P$ -value  $> 0.05$  and were not considered significant. (d) Endogenous expression of HilA-bmK-HA mutants in *S. Typhimurium*. *S. Typhimurium* HilA-HA strain (wt) and amber codon mutants (HilA-TAG-HA) with amber codon suppression system were grown with or without 100  $\mu$ M bmK. Anti-HA immunoprecipitated samples were analyzed with SDS-PAGE in-gel fluorescence scanning (top) and anti-HA immunoblotting. Also see Supplementary Fig. 14. (e) Secreted proteins of *S. Typhimurium* endogenous HilA-bmK-HA mutants. *S. Typhimurium* HilA-HA strain (wt) and amber codon mutants (HilA-TAG-HA) with amber codon suppression system were grown with or without 100  $\mu$ M bmK. Supernatants of the cultures were precipitated with 10% trichloroacetic acid (TCA) and analyzed with SDS-PAGE Coomassie blue staining.

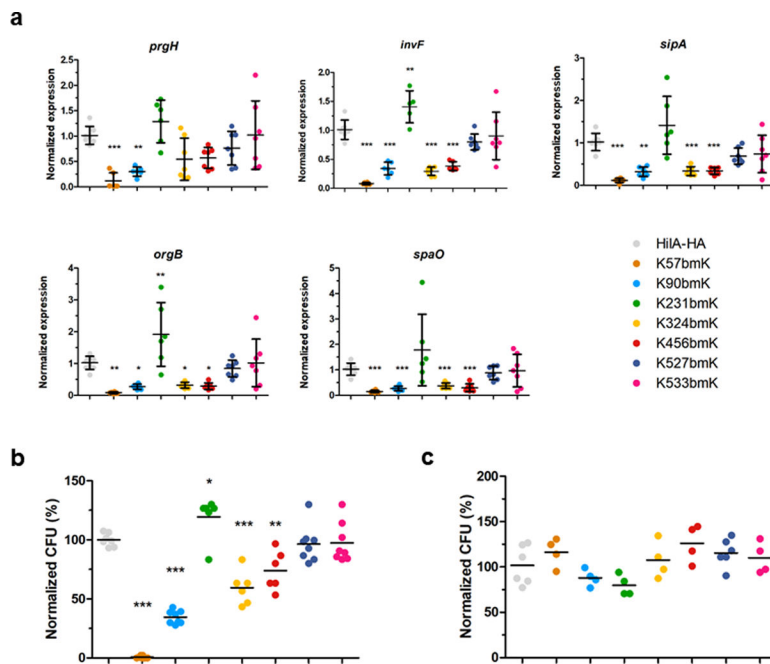


**Figure 3. Site-specific acylation of HilA affects *S. Typhimurium* transcriptional activity and invasion *in vitro*.**

(a) Relative expression level of SPI-1 genes in several operons (*prgH*, *invF*, *sipA*, *orgB*, and *spaO*) in *S. Typhimurium* HiIa-HA strains and HiIa-bmK-HA mutants measured by qRT-PCR ( $n = 6-8$ ). All mutants were compared to HiIa-HA with one-way ANOVA and Dunnett post-test. Centerline, average. Error bar, SD. \*,  $P$ -value < 0.05; \*\*,  $P$ -value < 0.01; \*\*\*,  $P$ -value < 0.001. Comparisons with no asterisk had  $P$ -value > 0.05 and were not considered significant. (b and c) Gentamicin protection assay of *S. Typhimurium* endogenous HiIa-bmK-HA mutants infecting HeLa cells (b) or RAW264.7 macrophages (c) at MOI = 10 ( $n = 4-8$ ). All mutants were compared to HiIa-HA with one-way ANOVA and Dunnett post-test. Centerline, average. \*,  $P$ -value < 0.05; \*\*\*,  $P$ -value < 0.001. Comparisons with no asterisk had  $P$ -value > 0.05 and were not considered significant.

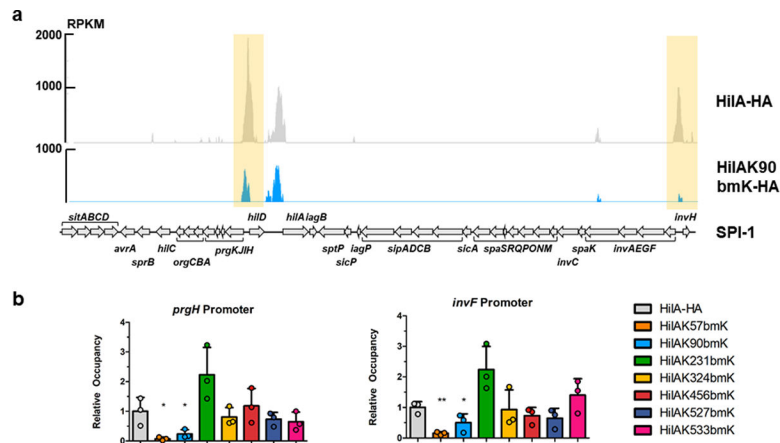


**Figure 4. HilAK90 acylation affects its occupancy at target genes.**

(a) Crosslink-IP-Seq result on *S. Typhimurium* HilA-HA and *S. Typhimurium* HilA-K90bmK-HA in SPI-1 region. Yellow shade, *prgH* promoter region (left) and *invF* promoter region (right). RPKM, Reads Per Kilobase Million. (b) Crosslink-IP-qPCR of *prgH* promoter region (left) or *invF* promoter region (right) of *S. Typhimurium* endogenous HilA-bmK-HA mutants ( $n = 3$ ). All mutants were compared to HilA-HA with one-way ANOVA and Dunnett post-test. Error bar, SD. \*,  $P$ -value  $< 0.05$ ; \*\*,  $P$ -value  $< 0.01$ . Comparisons with no asterisk had  $P$ -value  $> 0.05$  and were not considered significant.

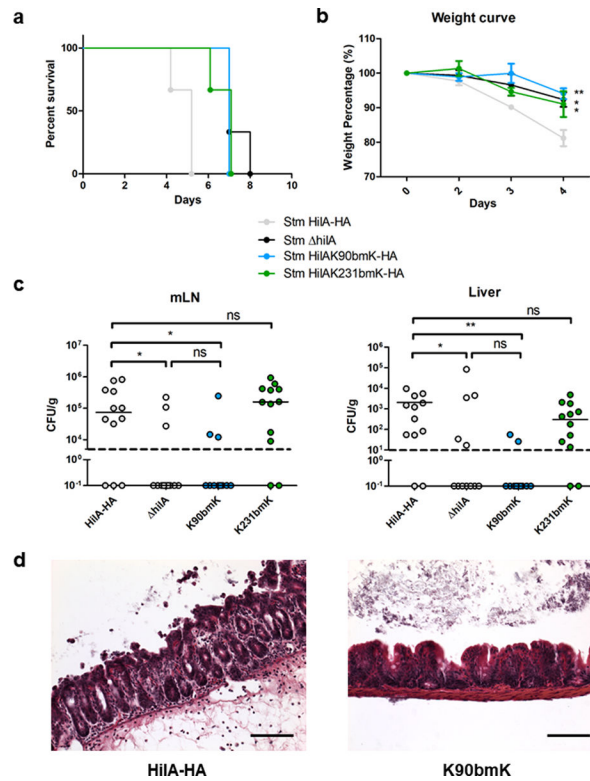


**Figure 5. HilAK90 acylation affects *S. Typhimurium* infection and intestinal inflammation *in vivo*.**

(a and b) C57BL/6 mice were orally infected with  $10^6$  CFU *S. Typhimurium* HilA-HA strain, *hilA* strain, HilAK90bmK-HA or HilAK231bmK-HA mutant ( $n = 3$ ). (a) survival and (b) weight loss are shown. Weights of all mutants at day 4 were compared to HilA-HA with one-way ANOVA and Dunnett post-test. Error bar, SD. \*,  $P$ -value < 0.05; \*\*,  $P$ -value < 0.01. (c) *S. Typhimurium* bacterial CFU counted from mesenteric lymph nodes (mLN, left) or liver (right) of mice orally infected with *S. Typhimurium* HilA-HA, *hilA*, HilA-K90bmK-HA or HilA-K231bmK-HA at 48h post-infection ( $n = 12$ ). HilA-K90bmK-HA and HilA-K231bmK-HA mutants were compared to HilA-HA or *hilA* with Kruskal-Wallis test and Dunns post-test. Centerline, median. \*,  $P$ -value < 0.05; \*\*,  $P$ -value < 0.01. ns, not significant. Dashed line, detection limit. (d) Representative images of cecum tissue stained with H&E, harvested 48h post-infection from mice infected with *S. Typhimurium* HilA-HA or HilA-K90bmK-HA. Scale bar, 100  $\mu$ m.

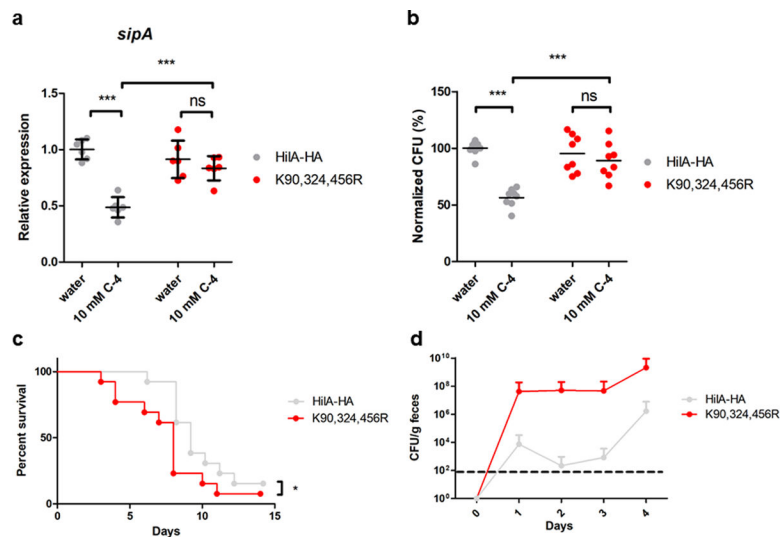


**Figure 6. HilA-K90,324,456R mutant resists butyrate inhibition *in vitro* and *in vivo*.**

(a) Relative expression level of SPI-1 gene *sipA* in *S. Typhimurium* HilA-HA strains and HilA-K90,324,456R-HA mutant in the presence or absence of 10 mM butyrate measured by qRT-PCR ( $n = 6$ ). Mutants were compared with one-way ANOVA and Bonferroni post-test. Centerline, average. Error bar, SD. \*\*\*,  $P$ -value  $< 0.001$ . ns, not significant. (b) Gentamicin protection assay of *S. Typhimurium* HilA-HA strains and HilA-K90,324,456R-HA mutant in the presence or absence of 10 mM butyrate infecting HeLa cells at MOI = 10 ( $n = 8$ ). Mutants were compared with one-way ANOVA and Bonferroni post-test. Centerline, average. Error bar, SD. \*\*\*,  $P$ -value  $< 0.001$ . ns, not significant. (c) Survival curve of C57BL/6 mice orally infected with  $10^6$  CFU *S. Typhimurium* HilA-HA or K90,324,456R mutant ( $n = 13$ ). Groups were compared with Gehan-Breslow-Wilcoxon test. \*,  $P$ -value  $< 0.05$ . (d) *S. Typhimurium* fecal load of mice as in (c). Error bar, SD. Dashed line, detection limit.